Tanaka,N.G., Sakamoto,N., Inoue,K., Korenaga,H., Kadoya,S., Ogawa,H. and Osada,Y. (1989) *Cancer Res.*, **49**, 6727–6730.

Ueba,T., Takahashi,J.A., Fukumoto,M., Ohta,M., Ito,N., Oda,Y., Kikuchi,H. and Hatanaka,M. (1994) *Neurosurgery*, **34**, 221–225; discussion 225–226.

Vitetta,E.S., Thorpe,P.E. and Uhr,J.W. (1993) *Immunol. Today*, **14**, 252–259.

Wu,Y., Saxena,S.K., Ardelt,W., Gadina,M., Mikulski,S.M., De Lorenzo,C., D'Alessio,G. and Youle,R.J. (1995) *J. Biol. Chem.*, **270**, 17476–17481.

Received December 7, 2004; revised April 21, 2005; accepted May 18, 2005

Edited by Dario Neri

JOURNAL OF BIOSCIENCE AND BIOENGINEERING
Vol. 99, No. 2, 95–103. 2005
DOI: 10.1263/jbb.99.095

ACCELERATED PUBLICATION

Intracellular Delivery of Proteins into Mammalian Living Cells by Polyethylenimine-Cationization

JUNICHIRO FUTAMI,[1,2] MIDORI KITAZOE,[1] TAKASHI MAEDA,[1] EMIKO NUKUI,[1] MASAKIYO SAKAGUCHI,[3] JUN KOSAKA,[4] MASAHIRO MIYAZAKI,[3] MEGUMI KOSAKA,[1] HIROKO TADA,[1] MASAHARU SENO,[1,5] JUNZO SASAKI,[4] NAM-HU HUH,[3] MASAYOSHI NAMBA,[6] AND HIDENORI YAMADA[1]*

Department of Bioscience and Biotechnology, Faculty of Engineering, Graduate School of Natural Science and Technology, Okayama University, Okayama 700-8530, Japan,[1] Nippon Shokubai Co., Ltd., 5-8 Nishi Otabi-cho, Suita, Osaka 564-8512, Japan,[2] Department of Cell Biology, Okayama University Graduate School of Medicine and Dentistry, Okayama 700-8558, Japan,[3] Department of Cytology and Histology, Okayama University Graduate School of Medicine and Dentistry, Okayama 700-8558, Japan,[4] Research Center for Biomedical Engineering, Okayama University, Okayama 700-8530, Japan,[5] and Niimi College, Niimi, Okayama 718-8585, Japan[6]

Received 6 December 2004/Accepted 15 December 2004

In the post-genomic era, there is pressing need for development of protein manipulation methodology to analyze functions of proteins in living cells. For this purpose, techniques to deliver functional proteins into living cells are currently being evaluated as alternative approaches to the introduction of transcriptionally active DNA. Here, we describe a novel method for efficient protein transduction into living cells in which a protein is simply cationized with polyethylenimine (PEI) by limited chemical conjugation. PEI-cationized proteins appear to adhere to the cell surface by ionic charge interaction and then internalize into cells in a receptor- and transporter-independent fashion. Since PEI is an organic macromolecule with a high cationic-charge density, limited coupling with PEI results in endowment of sufficient cationic charge to proteins without causing serious decline in their fundamental functions. A number of PEI-cationized proteins, such as ribonuclease (RNase), green fluorescent protein (GFP) and immunoglobulin (IgG), efficiently entered cells and functioned in the cytosol. Our results suggest that protein cationization techniques using PEI will be useful for the development of protein transduction technology.

[**Key words:** protein transduction, polyethylenimine (PEI), cationization, chemical modification, endocytosis]

Protein transduction, an efficient method for delivery of proteins into living cells, has many potential applications that range from basic study of protein function to development of novel therapeutics. Recent progress in protein transduction technology is promising for such purposes. Small cationic regions of proteins, called cell-penetrating peptides or protein transduction domains (PTD) such as human immunodeficiency virus TAT-(48-60), Antenapedia-(43-58) or Arg-rich peptides are among the most well-known peptides for these purposes (1–6). By attaching these carrier peptides, efficient protein transduction of $p16P^{INK4}$ (7), $p27P^{Kip1}$ (8), p53 (9), an HIV protease-activated caspase-3 (10) and Cre recombinase (11) *in vitro* and/or *in vivo* has been demonstrated to enable modulation of cellular events.

Although the mechanism remains controversial, the efficiency of PTD-mediated protein transduction is probably controlled by cell surface adsorption by ionic charge interaction between anionic cellular surface and cationic region of proteins (12–14), and that interaction appears to be followed by internalization through a caveolar endocytotic pathway (15). Likewise, highly cationic proteins, such as human eosinophile cationic protein (pI=11.9) (16) and artificially cationized proteins (17–26), have also shown efficient intracellular delivery. It was proposed more than a decade ago protein cationization is applicable to intracellular protein delivery by adsorption-mediated endocytosis (17, 18). This protein cationization method is accomplished by extensive amidation of carboxyl groups with various diamines (*e.g.*, ethylenediamine, Fig. 1A). Recently, we have demonstrated that non-toxic secretory RNases are converted to highly cytotoxic ones by cationization with ethylenediamine (25). Although these cationized RNases show markedly decreased enzymatic activity because of extensive modification of carboxyl groups, acquirement of a new function to pass through the cell membrane contributed to their cyto-

* Corresponding author. e-mail: yamadah@cc.okayama-u.ac.jp
phone: +81-(0)86-251-8215 fax: +81-(0)86-251-8265

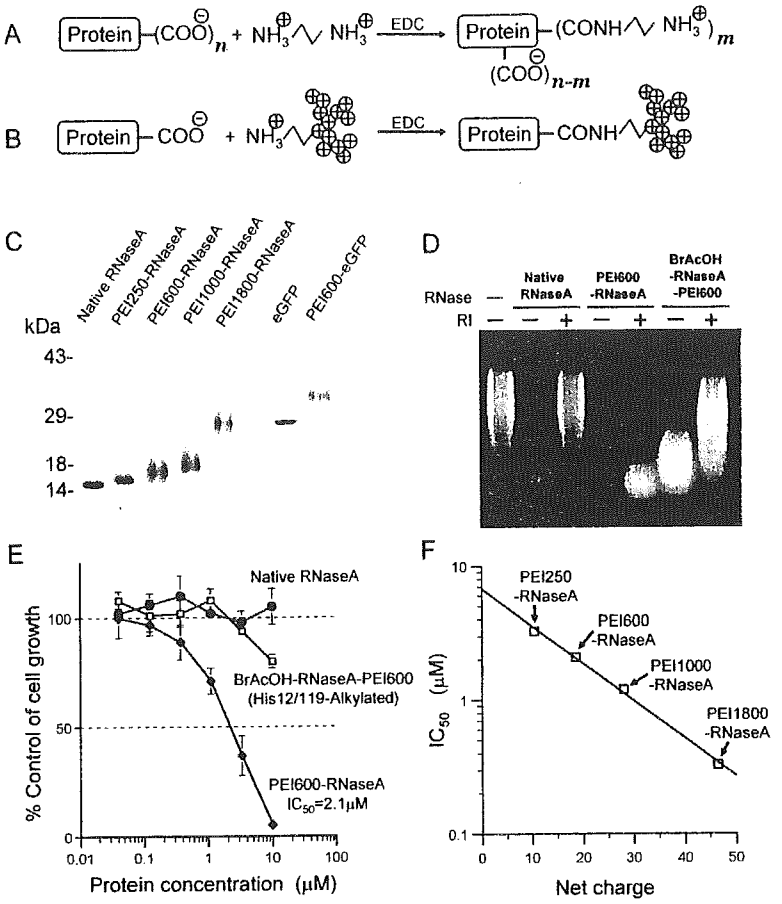

FIG. 1. Preparation and characterization of PEI-cationized proteins. Schema of protein cationization by amidation of the carboxyl group with ethylenediamine (A) and PEI (B) by a carbodiimide reaction. (C) SDS–PAGE analysis under reducing conditions using 15% polyacrylamide gel. (D) Agarose gel-based assay of enzymatic activity and RNase inhibitor resistance of RNases. *E. coli* ribosomal RNA was treated with 10 ng of RNases in the presence or absence of 10 molar excess RNase inhibitor for 15 min at 37°C, and then analyzed. (E) Cytotoxicity of RNases against Swiss 3T3-SV40 cells determined by an MTT assay after 3-d incubation. (F) Correlation between cytotoxic activity and net-charge of PEI-cationized RNaseA's.

toxicity. Thus, cationization of proteins with diamines is considered to be a powerful strategy to promote their internalization. However, unfavorable effects on protein function and stability due to the required extensive modification of carboxyl groups with diamines may limit its application (26).

In this report, we describe a new protein transduction method, cationization with polyethylenimine (PEI). PEI allows a protein to be more efficiently cationized than diamine and to maintain protein function as much as possible by a limited chemical conjugation (Fig. 1B). PEI, a polycationic polyamine, is a polymer with a branched backbone of two carbons followed by one potentially protonated nitrogen atom in every molecular mass unit of 43. PEIs with various molecular masses, ranging on average from 250 to 70,000, are available. Since PEI is toxicologically safe, it has been used as a food additive. Recently, PEI-mediated gene transfection by formation of a PEI/DNA noncovalent complex has been developed as a possible alternative to viral and liposomal routes of gene delivery (reviewed in Refs. 27–29).

Our experiments showed that a number of PEI-cationized proteins were efficiently delivered into living cells both *in vitro* and *in vivo*. Our results suggest that in addition to current PTD-fusion methodologies, the covalent conjugation of PEI to proteins is also a possible approach in protein transduction methodology for analyzing protein function in living cells or for specific manipulation of cellular events.

MATERIALS AND METHODS

Materials PEIs with various molecular masses (Epomin™ SP series: manufactured by Nippon Shokubai, Osaka) were donated by Nippon Shokubai or purchased from Wako Chemical (Osaka). The average molecular masses of PEIs (250, 600, 1000 and 1800) were used for their designations such as PEI600 in the text. 1-Ethyl-3-[3-(dimethylamino)propyl]carbodiimide hydrochloride (EDC) was purchased from Pierce (Rockford, IL, USA). Bovine RNaseA (Type XII-A), deoxyribonuclease (DN-25), holotransferrin and Rhodamine B isothiocyanate (RITC) were obtained from Sigma (St. Louis, MO, USA). Bafilomycin A1, Fluorescein isothiocyanate (FITC) and recombinant human RNase inhibitor were purchased from Wako Chemical. Preparation of rabbit antibody against human S100C was described previously (30).

Preparation of recombinant proteins Complementary

DNAs of His-tagged eGFP (eGFP) and TAT-eGFP fusion proteins, whose sequences were consistent with those previously reported (3), were subcloned into the pET14b vector (Novagen, WI, USA). Fusion proteins were expressed in transformed *Escherichia coli* BL21(DE3) pLysS. Each transformant was grown in terrific broth containing ampicillin (400 $\mu g \cdot ml^{-1}$) at 37°C. When an A_{600} of 1.0 was reached, culture media were cooled down to 25°C and added 0.5 mM of isopropyl 1-thio-β-D-galactopyranoside. After cultivation for further 16 h at 25°C, cells were harvested and frozen at −80°C. Frozen cells were thawed and homogenated in lysis buffer consisting of 20 mM Tris-HCl, pH 7.5, 20% sucrose, 0.2 M NaCl, 10 mM $MgCl_2$, and 30 $\mu g \cdot ml^{-1}$ of deoxyribonuclease. The suspension was followed by freeze-and-thaw for complete lysis and sonicated to decrease viscosity. To remove the nucleic acids, PEI600 (10% solution that had been adjusted to pH 8 with HCl) was added slowly until final concentration to be 0.7% with stirring on ice. After 15 min of stirring on ice, the precipitates were removed by centrifugation at 10,000×*g* for 15 min. The expressed fusion proteins were fractionated from the supernatants by 40–80% of saturated ammonium sulfate precipitates. The fusion proteins were purified using a TALON Superflow metal affinity column (Clontech, CA, USA). eGFP and TAT-eGFP thus obtained were directly used for following experiments without processing of His-tag peptide.

Chemical modification and fluorescence-labeling To prepare the enzymatically inactive RNaseA, one of the catalytic histidine residues (either His12 or His119) of RNaseA was alkylated by bromoacetate (31). Fluorescence labeling reactions to make rhodamine-labeled PEI600-eGFP and holo-transferrin, or fluorescein-labeled-anti-S100C and fluorescein-labeled PEI600-anti-S100C were carried out according to the method described previously (25).

Coupling of PEI to protein Coupling reactions of proteins with amine nucleophiles by EDC were described previously (32). Briefly, a protein was dissolved at a concentration of 1 $mg \cdot ml^{-1}$ in PEI solution (60 $mg \cdot ml^{-1}$, pH adjusted to 5.0 with HCl). The reaction was initiated by adding solid EDC at 0.1 $mg \cdot ml^{-1}$ into the protein solution with stirring at room temperature. After incubation for 16 h, the solution was dialyzed against distilled water, and then cationized protein was purified by carboxylic cation-exchanger CM-Toyopearl 650 M (Tosoh, Tokyo) column chromatography. Protein cationization by PEI was verified by SDS–PAGE. Sensitivity to RNase inhibitor of both native and chemical modified RNase were assessed according to the method described previously (25).

Cell culture and cytotoxicity assay Murine fibroblasts Balb/c 3T3 (clone A31-K) (33) and Swiss 3T3-SV40 (Dainippon Pharmaceutical, Osaka) and human fibroblasts (KMS-6) (34) were cultured in Dulbecco's modified Eagle's medium (DMEM) supplemented with 10% fetal bovine serum (FBS) and 70 $\mu g \cdot ml^{-1}$ of kanamycin. Cytotoxicity assay of free PEI (pH was adjust to 7.5 by HCl) and PEI cationized RNaseA was conducted with Swiss 3T3-SV40 cells. The protocol for the cytotoxicity assay using 3-(4,5-dimethylthiazol-2-yl)-2,5-diphenyltetrazolium bromide (MTT; Sigma) (MTT assay) was described previously (25).

Protein transduction of PEI cationized eGFP To visualize cellular uptake of cationized protein, PEI600-eGFP, rhodamine-labeled PEI600-eGFP or TAT-eGFP was directly added at 100 nM into culture media (DMEM supplemented with 10% FBS) of 70% confluent murine fibroblasts in 35-mm diameter glass base dishes. After incubation for various periods at 37°C, fluorescence images were directly analyzed using a laser scanning confocal microscope (model MRC-1024; Bio-Rad Laboratories, Hercules, CA, USA). To examine colocalization of PEI600-eGFP and RITC-transferrin, the mixture of them was added at 100 nM each to exponentially growing murine fibroblasts on a glass coverslip in serum-free DMEM for 90 min at 37°C. After wash with serum-free DMEM, fluorescence images were directly analyzed using a confocal laser-scanning microscope (LSM 510 META; Carl Zeiss, Jena, Germany) using a ×63 oil-immersion objective without fixation.

Protein transduction of PEI cationized antibody To analyze intracellular distribution of PEI-cationized antibody, exponentially growing KMS-6 cells on a glass coverslip were incubated with fluorescein-labeled PEI600-anti-S100C in serum-free DMEM for 3 h at 37°C. Cells were then washed with fresh serum-free medium and cultured again for 24 h in the absence of the cationized antibody. After wash with PBS, fluorescence images were directly analyzed using a confocal laser-scanning microscope (LSM 510 META) without fixation. Subsequently, cells were fixed with 4% paraformaldehyde and analyzed again.

Flow cytometry Exponentially growing Balb/c 3T3 cells were incubated with 100 nM of PEI600-eGFP or TAT-eGFP in DMEM supplemented with 10% FBS. After incubation for 24 h at 37°C, the cells were washed with PBS, dissociated with trypsin and analyzed by fluorescence flow cytometry (FACS). To test the stability of transiently transduced protein in Balb/c 3T3 cells, cells treated with 100 nM of PEI600-eGFP for 24 h were washed three times with PBS and cultured again in the absence of PEI600-eGFP. After incubation for 0, 24 and 48 h, the cells were analyzed by FACS as described above, respectively.

Animal study C57BL/6 mice (8 weeks old) were each injected intraperitoneally with 300 μg of PEI600-eGFP dissolved in 0.9% NaCl solution. After 8 h, the mice were sacrificed and their tissues were harvested. Isolated tissues were quickly frozen in Tissue-Tek (Miles Scientific, Naperville, IL, USA). Anesthetized male Wistar rats (8 weeks old) were each injected intraportally with 100 μg of PEI600-eGFP in 0.9% NaCl solution. After 1 h, the livers were resected and frozen as described above. Ten-μm-thick sections were prepared on a cryostat and analyzed under a fluorescence microscope. The treatment of all animals was performed strictly in accordance with the institutional and National Institutes of Health (NIH) guidelines for care and treatment of laboratory animals.

RESULTS

Protein transduction of PEI-cationized RNases The first model study to evaluate the protein transduction ability of PEI was conducted using 14-kDa bovine RNaseA, which should exhibit cytotoxic effects when it internalizes into cells (35). PEIs with molecular masses of 250, 600, 1000 and 1800 were coupled to RNaseA by a carbodiimide reaction (Fig. 1B), and then each 1:1 PEI-RNaseA conjugate was purified by carboxylic cation-exchange chromatography, respectively. All conjugates of PEI-RNaseA thus prepared (Fig. 1C) showed 20–28% ribonucleolytic activity of native RNaseA and they were highly cytotoxic to murine fibroblast Swiss 3T3-SV40 cells (IC_{50}=0.3 to 3.0 μM, Table 1). Because mammalian cells are ubiquitously expressing cytosolic RNase inhibitor (36), the sensitivity of endogenous RNase inhibitor to internalized RNase is one of the limitation factors for RNase cytotoxicity (25, 26, 37). As shown in Fig. 1D, PEI600-RNaseA showed markedly decreased interaction to RNase inhibitor (Fig. 1D), suggesting that the coupling of PEIs to RNaseA on a molecular surface endowed it with both cell-penetrating domain and possible steric hindrance to the interaction with endogenous RNase inhibitor.

In order to exclude a possible influence of non-specific cytotoxicity of the PEI-cationized protein, almost inactive PEI600-cationized RNaseA (<0.05%), which has catalytic

TABLE 1. Charcteristics of PEI-cationized RNaseA derivatives and free PEI

Molecule	Estimated net charge[a]	RNase activity[b] (%)	IC_{50}[c] (μM)
Native RNaseA	+4	100	>100
PEI250-RNaseA	+10.4	22	3.3
PEI600-RNaseA	+18.6	20	2.1
PEI1000-RNaseA	+27.9	28	1.2
PEI1800-RNaseA	+46.5	27	0.33
BrAcOH-RNaseA-PEI600	+17.6	<0.05	>100
PEI250	+6.4	–	>1000
PEI600	+14.6	–	1000
PEI1000	+23.9	–	200
PEI1800	+42.5	–	20

[a] The net charge of molecule at neutral pH was estimated from the amino acid composition of RNaseA and the molecular mass of PEI which has (molecular mass +26)/43 of potentially protonated nitrogen atoms per molecule.

[b] Relative RNase activity determined against yeast RNA according to the methods described elsewhere (44).

[c] The concentration required for inhibition of 50% of the growth of 3T3-SV40 cells at 37°C for 3 d.

residue (either His12 or His119) alkylated with bromoacetate, was used as negative control. No obvious cytotoxicity was observed in inactive PEI600-cationized RNaseA and PEI molecules themselves as well (Table 1 and Fig. 1E).

As observed in RNaseA derivatives extensively modified with taurine, ethanolamine, and ethylenediamine (25), cytotoxicity of PEI-cationized RNaseA was also well related to the protein net positive charge (Table 1 and Fig. 1F). Moreover, when in the presence of an anionic polymer of heparin, the cytotoxicity of PEI-RNaseA was efficiently abolished (data not shown). These results suggest that the crucial step for cellular uptake of PEI-cationized protein is determined by the efficiency of electrostatic adsorption to the anionic cellular surface.

Previously, we have shown that RNaseA extensively cationized with ethylenediamine (Fig. 1A) showed equivalent cytotoxicity (IC_{50}=0.17 μM) but a remarkable decrease in ribonucleolytic activity (1.6%) (25). This means that to avoid loss of protein function as much as possible at the same level of cationization, the limited coupling with PEI is superior to the extensive coupling with ethylenediamine.

Protein transduction of PEI-cationized eGFP The second model protein, 29-kDa enhanced green fluorescent protein (eGFP), was coupled to PEI by the carbodiimide reaction (Fig. 1B) to visualize cellular uptake of PEI-cationized protein. In the preliminary study, we have prepared eGFP coupled to various molecular mass (300, 600, 1000, 1200 and 1800) of PEIs and observed their protein transduction efficiency. Although all PEI-cationized eGFPs were successfully transduced to cells, the fluorescent image due to intracellular distribution of PEI600-eGFP seemed to be the best (data not shown). PEI600-eGFP conserved more than 90% of the original fluorescent emission intensity. In contrast, eGFP, which was extensively cationized with ethylenediamine (Fig. 1A), showed a remarkable decrease in fluorescence (about 35%). To test internalization of PEI-cationized proteins into cells, 100 nM of PEI600-eGFP was added to each culture medium of murine fibroblast Swiss 3T3-SV40 cells, and the cells were observed under a confocal microscope in order to scan the internalized PEI600-eGFP but not the one attached to the plasma membrane. As shown in Fig. 2A, PEI600-eGFP was rapidly incorporated into cells, and all of the cultured cells emitted green fluorescence due to internalized exogenous eGFP. The amount of intracellular PEI600-eGFP appeared to increase in a time-dependent fashion (Fig. 2A).

Comparison of protein transduction efficiency between PEI600-eGFP and TAT-eGFP We constructed a TAT-eGFP fusion protein by connecting the TAT transduction domain to the N-terminus of eGFP and added the fusion protein to cultures of Swiss 3T3-SV40 cells. Confocal microscopic analysis showed the presence of TAT-eGFP fusion protein in the cytoplasm of Swiss 3T3-SV40 cells, but the fluorescence intensity of TAT-eGFP in the cells was far lower than that of PEI600-eGFP in spite of similar intrinsic fluorescence intensities in both proteins (data not shown). For further detailed comparison, 100 nM of PEI600-eGFP or TAT-eGFP was added to each culture of murine fibroblast Balb/c 3T3 cells. After incubation for 24 h, the cells were then analyzed by FACS. Although the cellular fluorescence in this assay included both cell surface and intracellular fractions, the fluorescence of PEI600-eGFP-treated cells was more than 100-fold greater than that of TAT-eGFP-treated cells (Fig. 2B).

Destination of transiently transduced PEI600-eGFP in living cells To test the stability of transiently transduced protein in murine fibroblast Balb/c 3T3 cells, cells treated with 100 nM of PEI600-eGFP for 24 h as above were washed three times with phosphate-buffered saline (PBS) and cultured again in the absence of PEI600-eGFP. The fluorescence of eGFP showed a time-dependent decrease but was detectable even after 48 h (Fig. 2C). Fairly narrow distribution of PEI600-eGFP-treated cells indicated that individual cells within each population contained a statistically distributed similar amount of eGFP moiety. These results suggest that internalized PEI600-eGFP may be gradually degraded in cells.

Analysis of cellular uptake route of PEI600-eGFP Since fluorescence of eGFP is very sensitive to pH, it can be used as an intracellular pH indicator in living cells (38). The p*Ka* of PEI600-eGFP was 5.6 as determined by a titration sigmoidal curve, indicating that eGFP fluorescence disappears at acidic organelles such as late-endosome or lysosome. To chase internalized PEI600-eGFP independently, rhodamine-labeled PEI600-eGFP was prepared. When cells were treated with rhodamine-labeled PEI600-eGFP, accumulation of the fluorescence due to only rhodamine but not eGFP was evidently detected within cells by confocal microscopy (Fig. 3A, upper panels). In contrast, the confocal microscopic images showed that the eGFP fluorescence did not diminish in the cells in which acidification of late-endosome and lysosome was inhibited by the proton pump inhibitor bafilomycin A1 (H^+ v-ATPase inhibitor) (39) (Fig. 3A, lower panels). These observations suggest that one of the major uptake routes of PEI-cationized protein is an internalization via a non-specific cellular surface adsorption-mediated endocytosis. Furthermore, intracellular endosomes containing PEI-cationized protein were clearly distinguish-

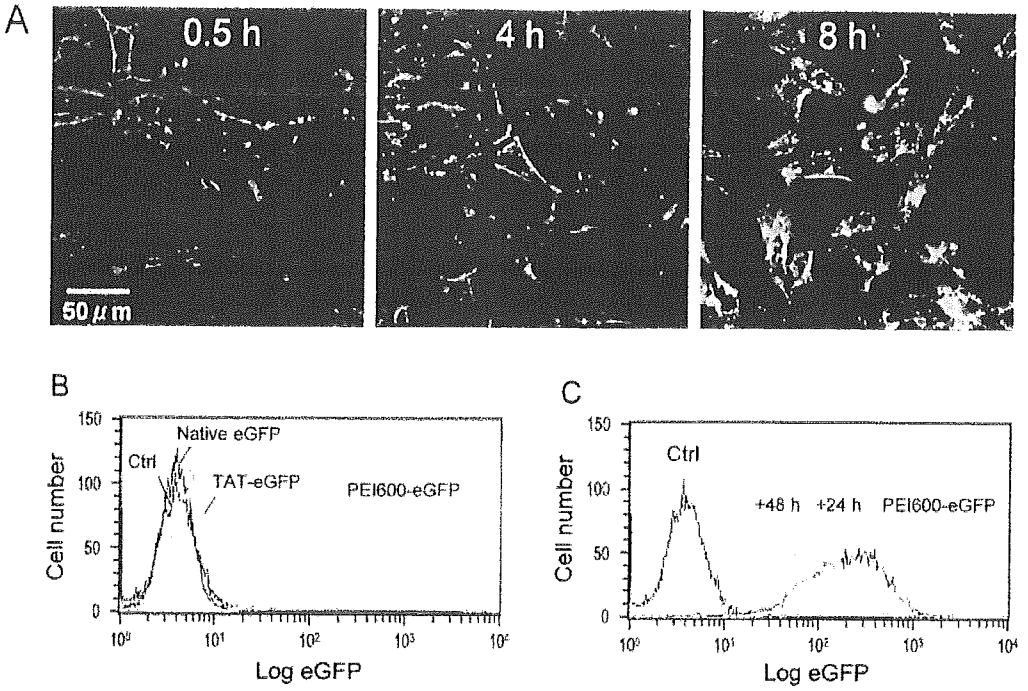

FIG. 2. Internalization and degradation of PEI-cationized eGFP into murine fibroblast. (A) Time course of PEI600-eGFP internalization into Swiss 3T3-SV40 cells analyzed under a confocal microscope without fixation. (B) FACS analysis of Balb/c 3T3 cells after treatment with 100 nM native eGFP, TAT-eGFP or PEI600-eGFP for 24 h. (C) FACS kinetic analysis of Balb/c 3T3 cells that had been transduced with PEI600-eGFP for 24 h (same as green in panel B) and then washed and cultured again in the absence of the cationized eGFP for a further 24 or 48 h. All experiments were performed using DMEM supplemented with 10% FBS.

able from the transferrin-receptor mediated ones (Fig. 3B).

Protein transduction of PEI-cationized antibody

For the third model protein, a 150-kDa immunoglobulin (IgG) was delivered into living cells by PEI-cationazation method (Fig. 1B). To demonstrate the functionality of intracellular protein delivery by PEI-cationization, we chose to examine visualization of antigen protein in living cell. Rabbit antibody against human S100C, a protein that has been found to be decreased in immortalized human fibroblasts and to bind actin filaments, was used in this assay (30). To examine PEI-cationized IgG protein transduction, KMS-6 cells were incubated with FITC-labeled PEI600-anti-S100C IgG or FITC-labeled PEI600-control IgG under serum-free conditions as described in Materials and Methods. Figures 4A and 4B show the intracellular distributions of PEI600-control IgG and PEI600-anti-S100C antibody, respectively. As shown in Fig. 4B, PEI600-anti-S100C antibody was localized in the cytoplasm showning a cytoskeletal-like structure. When the FITC-labeled PEI600-anti-S100C antibody were added to KMS-6 cells in the presence of 10% FBS, bright fluorescence of punctuate structures interfered with observing of cytoskeletal-like structures (data not shown). Serum seemed to enhance endocytotic activity of cells. These results strongly suggest that PEI-cationized antibody can internalize into living cells and properly localize on its target antigen and the reduction of background, bright fluorescence of endsome-like vesicular structures, by incubation without serum may be important for imaging intracellular antigen.

Recently, we have demonstrated that the intracellular delivery of PEI-cationized anti-S100C antibody into living normal human keratinocyte resulted in successful neutralization of S100C Ca^{2+}-induced phosphorylation (40). Together with the results described above, it is concluded that PEI-cationized IgGs enter into living cells and would bind to the exact antigen if accessible.

Protein transduction of PEI-cationized eGFP *in vivo*

To determine whether PEI-cationized protein could be transduced *in vivo*, we intraperitoneally and intraportally injected PEI600-eGFP into mice and rats, respectively, and then analyzed fluorescence of eGFP in their tissue sections. As shown in Fig. 5A, PEI600-eGFP had accumulated on the kidney surface at 8 h after intraperitoneal injection. Similar results were obtained by observation of the peritoneum (Fig. 5B) and the liver (Fig. 5C). In contrast, PEI600-eGFP had preferentially accumulated around the hepatic portal vein in the liver at 1 h after intraportally injection (Fig. 5D). On the other hand, when control native eGFP was injected *in vivo*, such fluorescence was not observed (data not shown). These results indicate that PEI-cationized protein was transduced into cells *in vivo* via a principally cellular surface adsorption-mediated process.

DISCUSSION

PEI-RNaseAs were cytotoxic (Fig. 1 and Table 1), PEI600-eGFP showed bright intracellular fluorescence (Figs. 2 and 5), and FITC-PEI600-anti-S100C antibody gave the fluorescence image of intracellular cytoskeletal-like structure (Fig. 4). All of these results indicate that PEI-cationization

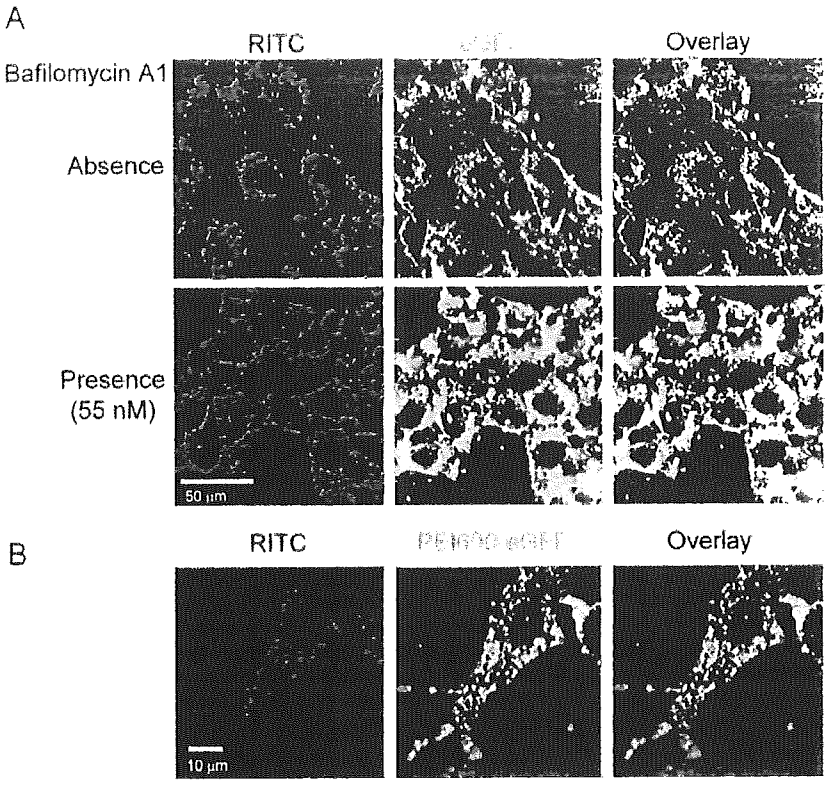

FIG. 3. Analysis of internalization of PEI-cationized eGFP and transferrin into Balb/c 3T3 cells through endcytosis. Intracellular delivery route of PEI-cationized protein was analyzed in Balb/c 3T3 cells by incubation of the cells with 100 nM rhodamine-labeled PEI600-eGFP for 24 h in the absence (A, upper panels) or presence of 55 nM bafilomycin A1 (A, lower panels). Balb/c 3T3 cells were co-incubated with 100 nM each of PEI600-eGFP and RITC-transferrin for 90 min in the absence of serum. Note the distinct locations of two proteins internalized into cells (B).

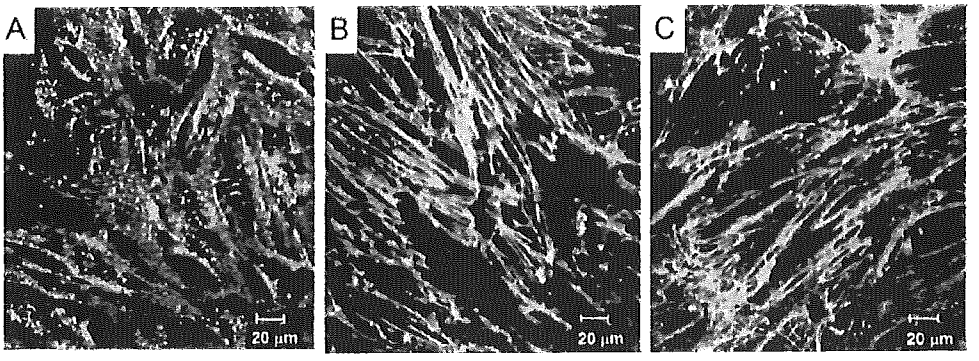

FIG. 4. Protein transduction of PEI-cationized antibody into living human fibroblast KMS-6 cells. Rabbit anti-human S100C IgG or non-immunized IgG was cationized with PEI600 and then labeled with FITC. When cells were treated with FITC-PEI600-anti-S100C IgG, fluorescence was detected along with cytoskeletal-like structure (B), whereas no such specific fluorescence pattern was detected in cells treated with FITC-PEI600-nonimmunized IgG (A). Fluorescence pattern along with cytoskeletal-like structure shown in panel B was not affected by paraformaldehyde fixation (C).

is one of the promising methods to introduce biologically active proteins into living cells both *in vitro* and *in vivo*. As yet, we have not encountered cells that refuse transduction of PEI-eGFP among several human carcinoma or leukemia derived cell lines, hematopoietic cells or primary culture of neural cells (unpublished observation). Thus, we concluded that PEI-cationized proteins can be delivered not only into every cultured cell at high level simply by adding them to the culture media, but also into living tissues from surface region by injecting them.

Almost all mammalian cell surfaces are composed of various glycoproteins (41) having antennary glycosyl chains with negatively charged terminal sialic acid residues (42, 43). Furthermore, entities of biological membrane are also negatively charged because of acidic phospholipids such as phosphatidylglycerol. The cell membrane is continuously internalized into cells by constitutive endocytosis. Proteins adhering to the cell surface will accordingly also become in-

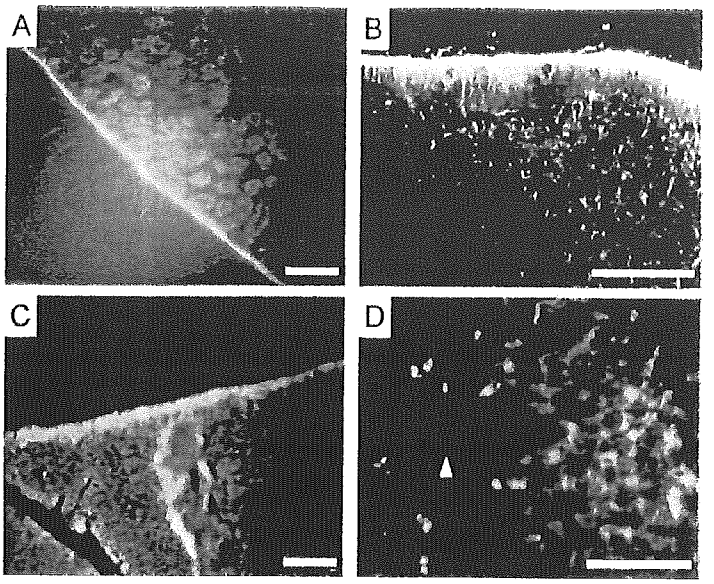

FIG. 5. Protein transduction of PEI-cationized eGFP *in vivo*. Transduction of PEI600-eGFP in mice (A–C) and rats (D) were analyzed by fluorescence micrograph tissue sections. Strong fluorescence is observed in surface areas of the mouse kidney (A), peritoneum (B) and liver (C) at 8 h after intraperitoneal injection of PEI600-eGFP. Intraportally injected PEI600-eGFP appeared in the rat liver at 1 h after injection. Gradient fluorescence is observed in hepatic cells from the hepatic portal vein (right) to the central vein (arrow head) (D). Scale bars represent 50 μm.

ternalized into cells and end up in lysosome and other intracellular vesicles. Recent reports have shown that the protein transduction domains or cell penetrating peptides also mediate cell surface adhesion followed by internalization into cells by endocytosis (13, 14). Therefore, enhancement of the ionic charge interaction seems to be a reasonable strategy to increase the adsorption-mediated delivery of a protein into variety of cells.

We have recently observed that cationic net-charge of proteins correlated well with their efficiency of cell internalization when they were added to the culture media (16, 25, 26). These data are completely consistent with the present data (Fig. 1F). PEIs are the most suitable reagents to endow a protein with the highest cationic net-charge by the least coupling (Fig. 1B). For example, the net-charges of eGFP and TAT-eGFP used in this study are −7 and −3, respectively. Both proteins could not adhere to cellular surface (Fig. 2B). On the other hand, PEI600-eGFP with a cationic net-charge of $-7+14.6m$ (m: number of modified carboxyl group) showed drastically enhanced cellular surface adhesion and resulted in efficient protein transduction. In this study, we have employed limited PEI-cationization ($m=1\sim3$) because the over conjugation of PEI would result in dysfunction of protein. Furthermore, heavily cationized protein might seriously affect some cellular events when it adheres on plasma membrane. Thus, optimum level of cationization may have to be chosen to avoid unfavorable side effects on both protein and cell in this protein transduction method (26). Relatively low molecular mass of PEIs (PEI300–PEI1200) were considered to satisfy these requirements.

PEI has several advantages such as rapid and efficient delivery of proteins into cells, stability in physiological buffer, resistance to protease degradation, low degree of toxicity (Table 1), and low sensitivity to serum. The significance of stability of PTDs in culture media on their efficiency of intracellular delivery has been pointed out, because those consisting of D-form enhanced cellular uptake compared to protease sensitive L-form (4). The most prominent feature of PEI is its highest cationic charge density among existing polymers. PEI contains one possible positive charge (one protonatable nitrogen atom) in every repeating monomer molecular mass unit of 43, which is much smaller than that in Poly-Lys or Poly-Arg (129 or 157). For these reasons, PEI can be a suitable polymer as a cationic protein transduction domain.

Although PEI-cationization methods described in this paper is one of the powerful strategies to protein transduction, this method may not be generally available to use for the protein in short supply, or the proteins sensitive to chemical reaction like PEI-cationization. To escape these limitations, we are now improving the method using PEI-cationized carrier protein that can form complex to the protein to be delivered (unpublished).

The protein transduction technology provides several advantages over DNA transfection, the current standard method of intracellular protein expression. For example, the needed intracellular concentration depending on temporal requirement may be controlled just by varying the amount of a proteins added to culture medium. Furthermore, every cell in population appears to contain a near-identical intracellular concentration of the protein. As shown in Fig. 2C, transiently internalized protein is likely to be metabolized in biological process. Furthermore, PEI-cationized antibody successfully binds to target antigen in living cell (Fig. 4), suggesting that this technology may be applicable for intracellular antibody (intrabody) therapy.

In the past several years, a variety of applications using protein transduction technology have been demonstrated. These findings are now promising for their further development of their applications. As described here, high effi-

ciency of protein transduction based on PEI-cationization technology may pave the way of novel application ranging from basic study to novel protein therapeutics.

ACKNOWLEDGMENTS

We thank Dr. Masaki Hikida for performing the FACS. This work was performed as a part of a research and development project of the Industrial Science and Technology Program supported by the New Energy and Industrial Technology Development Organization (NEDO) and fellowships of Japan Society for the Promotion of Science, Japan.

REFERENCES

1. **Derossi, D., Joliot, A. H., Chassaing, G., and Prochiantz, A.:** The third helix of the Antennapedia homeodomain translocates through biological membranes. J. Biol. Chem., **269**, 10444–10450 (1994).
2. **Vivès, E., Brodin, P., and Lebleu, B.:** A truncated HIV-1 Tat protein basic domain rapidly translocates through the plasma membrane and accumulates in the cell nucleus. J. Biol. Chem., **272**, 16010–16017 (1997).
3. **Schwarze, S. R., Ho, A., Vocero-Akbani, A., and Dowdy, S. F.:** *In vivo* protein transduction: delivery of a biologically active protein into the mouse. Science, **285**, 1569–1572 (1999).
4. **Wender, P. A., Mitchell, D. J., Pattabiraman, K., Pelkey, E. T., Steinman, L., and Rothbard, J. B.:** The design, synthesis, and evaluation of molecules that enable or enhance cellular uptake: peptoid molecular transporters. Proc. Natl. Acad. Sci. USA, **97**, 13003–13008 (2000).
5. **Futaki, S., Suzuki, T., Ohashi, W., Yagami, T., Tanaka, S., Ueda, K., and Sugiura, Y.:** Arginine-rich peptides. An abundant source of membrane-permeable peptides having potential as carriers for intracellular protein delivery. J. Biol. Chem., **276**, 5836–5840 (2001).
6. **Matsushita, M., Tomizawa, K., Moriwaki, A., Li, S. T., Terada, H., and Matsui, H.:** A high-efficiency protein transduction system demonstrating the role of PKA in long-lasting long-term potentiation. J. Neurosci., **21**, 6000–6007 (2001).
7. **Gius, D. R., Ezhevsky, S. A., Becker-Hapak, M., Nagahara, H., Wei, M. C., and Dowdy, S. F.:** Transduced p16INK4a peptides inhibit hypophosphorylation of the retinoblastoma protein and cell cycle progression prior to activation of Cdk2 complexes in late G1. Cancer Res., **59**, 2577–2580 (1999).
8. **Nagahara, H., Vocero-Akbani, A. M., Snyder, E. L., Ho, A., Latham, D. G., Lissy, N. A., Becker-Hapak, M., Ezhevsky, S. A., and Dowdy, S. F.:** Transduction of full-length TAT fusion proteins into mammalian cells: TAT-p27Kip1 induces cell migration. Nat. Med., **4**, 1449–1452 (1998).
9. **Takenobu, T., Tomizawa, K., Matsushita, M., Li, S. T., Moriwaki, A., Lu, Y. F., and Matsui, H.:** Development of p53 protein transduction therapy using membrane-permeable peptides and the application to oral cancer cells. Mol. Cancer Ther., **1**, 1043–1049 (2002).
10. **Vocero-Akbani, A. M., Heyden, N. V., Lissy, N. A., Ratner, L., and Dowdy, S. F.:** Killing HIV-infected cells by transduction with an HIV protease-activated caspase-3 protein. Nat. Med., **5**, 29–33 (1999).
11. **Peitz, M., Pfannkuche, K., Rajewsky, K., and Edenhofer, F.:** Ability of the hydrophobic FGF and basic TAT peptides to promote cellular uptake of recombinant Cre recombinase: a tool for efficient genetic engineering of mammalian genomes. Proc. Natl. Acad. Sci. USA, **99**, 4489–4494 (2002).
12. **Suzuki, T., Futaki, S., Niwa, M., Tanaka, S., Ueda, K., and Sugiura, Y.:** Possible existence of common internalization mechanisms among arginine-rich peptides. J. Biol. Chem., **277**, 2437–2443 (2002).
13. **Richard, J. P., Melikov, K., Vives, E., Ramos, C., Verbeure, B., Gait, M. J., Chernomordik, L. V., and Lebleu, B.:** Cell-penetrating peptides. A reevaluation of the mechanism of cellular uptake. J. Biol. Chem., **278**, 585–590 (2003).
14. **Lundberg, M., Wikstrom, S., and Johansson, M.:** Cell surface adherence and endocytosis of protein transduction domains. Mol. Ther., **8**, 143–150 (2003).
15. **Fittipaldi, A., Ferrari, A., Zoppe, M., Arcangeli, C., Pellegrini, V., Beltram, F., and Giacca, M.:** Cell membrane lipid rafts mediate caveolar endocytosis of HIV-1 Tat fusion protein. J. Biol. Chem., **278**, 34141–34149 (2003).
16. **Maeda, T., Kitazoe, M., Tada, H., de Llorens, R., Salomon, D. S., Ueda, M., Yamada, H., and Seno, M.:** Growth inhibition of mammalian cells by eosinophil cationic protein. Eur. J. Biochem., **269**, 307–316 (2002).
17. **Kumagai, A. K., Eisenberg, J. B., and Pardridge, W. M.:** Absorptive-mediated endocytosis of cationized albumin and a beta-endorphin-cationized albumin chimeric peptide by isolated brain capillaries. Model system of blood-brain barrier transport. J. Biol. Chem., **262**, 15214–15219 (1987).
18. **Apple, R. J., Domen, P. L., Muckerheide, A., and Michael, J. G.:** Cationization of protein antigens. IV. Increased antigen uptake by antigen-presenting cells. J. Immunol., **140**, 3290–3295 (1988).
19. **Triguero, D., Buciak, J. B., Yang, J., and Pardridge, W. M.:** Blood-brain barrier transport of cationized immunoglobulin G: enhanced delivery compared to native protein. Proc. Natl. Acad. Sci. USA, **86**, 4761–4765 (1989).
20. **Triguero, D., Buciak, J. L., and Pardridge, W. M.:** Cationization of immunoglobulin G results in enhanced organ uptake of the protein after intravenous administration in rats and primate. J. Pharmacol. Exp. Ther., **258**, 186–192 (1991).
21. **Pardridge, W. M., Bickel, U., Buciak, J., Yang, J., and Diagne, A.:** Enhanced endocytosis and anti-human immunodeficiency virus type 1 activity of anti-rev antibodies after cationization. J. Infect. Dis., **169**, 55–61 (1994).
22. **Pardridge, W. M., Kang, Y. S., Yang, J., and Buciak, J. L.:** Enhanced cellular uptake and *in vivo* biodistribution of a monoclonal antibody following cationization. J. Pharm. Sci., **84**, 943–948 (1995).
23. **Pardridge, W. M., Buciak, J., Yang, J., and Wu, D.:** Enhanced endocytosis in cultured human breast carcinoma cells and *in vivo* biodistribution in rats of a humanized monoclonal antibody after cationization of the protein. J. Pharmacol. Exp. Ther., **286**, 548–554 (1998).
24. **Hong, G., Bazin-Redureau, M. I., and Scherrmann, J. M.:** Pharmacokinetics and organ distribution of cationized colchicine-specific IgG and Fab fragments in rat. J. Pharm. Sci., **88**, 147–153 (1999).
25. **Futami, J., Maeda, T., Kitazoe, M., Nukui, E., Tada, H., Seno, M., Kosaka, M., and Yamada, H.:** Preparation of potent cytotoxic ribonucleases by cationization: enhanced cellular uptake and decreased interaction with ribonuclease inhibitor by chemical modification of carboxyl groups. Biochemistry, **40**, 7518–7524 (2001).
26. **Futami, J., Nukui, E., Maeda, T., Kosaka, M., Tada, H., Seno, M., and Yamada, H.:** Optimum modification for the highest cytotoxicity of cationized ribonuclease. J. Biochem. (Tokyo), **132**, 223–228 (2002).
27. **Godbey, W. T., Wu, K. K., and Mikos, A. G.:** Poly(ethylenimine) and its role in gene delivery. J. Control. Release, **60**, 149–160 (1999).
28. **Lemkine, G. F. and Demeneix, B. A.:** Polyethylenimines for *in vivo* gene delivery. Curr. Opin. Mol. Ther., **3**, 178–182 (2001).
29. **Matsuura, M., Yamazaki, Y., Sugiyama, M., Kondo, M., Ori, H., Nango, M., and Oku, N.:** Polycation liposome-me-

diated gene transfer *in vivo*. Biochim. Biophys. Acta, **1612**, 136–143 (2003).
30. **Sakaguchi, M., Miyazaki, M., Inoue, Y., Tsuji, T., Kouchi, H., Tanaka, T., Yamada, H., and Namba, M.:** Relationship between contact inhibition and intranuclear S100C of normal human fibroblasts. J. Cell Biol., **149**, 1193–1206 (2000).
31. **Bello, J. and Nowoswiat, E. F.:** Multiple carboxymethylation of histidines in bovine ribonuclease A. Eur. J. Biochem., **22**, 225–234 (1971).
32. **Yamada, H., Imoto, T., Fujita, K., Okazaki, K., and Motomura, M.:** Selective modification of aspartic acid-101 in lysozyme by carbodiimide reaction. Biochemistry, **20**, 4836–4842 (1981).
33. **Peterkofsky, B. and Prather, W.:** Correlation between the rates of aerobic glycolysis and glucose transport, unrelated to neoplastic transformation, in a series of BALB 3T3-derived cell lines. Cancer Res., **42**, 1809–1816 (1982).
34. **Namba, M., Nishitani, K., Hyodoh, F., Fukushima, F., and Kimoto, T.:** Neoplastic transformation of human diploid fibroblasts (KMST-6) by treatment with 60Co gamma rays. Int. J. Cancer, **35**, 275–280 (1985).
35. **Rybak, S. M. and Newton, D. L.:** Natural and engineered cytotoxic ribonucleases: therapeutic potential. Exp. Cell Res., **253**, 325–335 (1999).
36. **Futami, J., Tsushima, Y., Murato, Y., Tada, H., Sasaki, J., Seno, M., and Yamada, H.:** Tissue-specific expression of pancreatic-type RNases and RNase inhibitor in humans. DNA Cell Biol., **16**, 413–419 (1997).
37. **Dickson, K. A., Dahlberg, C. L., and Raines, R. T.:** Compensating effects on the cytotoxicity of ribonuclease A variants. Arch. Biochem. Biophys., **415**, 172–177 (2003).
38. **Kneen, M., Farinas, J., Li, Y., and Verkman, A. S.:** Green fluorescent protein as a noninvasive intracellular pH indicator. Biophys. J., **74**, 1591–1599 (1998).
39. **Dröse, S. and Altendorf, K.:** Bafilomycins and concanamycins as inhibitors of V-ATPases and P-ATPases. J. Exp. Biol., **200 (Pt 1)**, 1–8 (1997).
40. **Sakaguchi, M., Miyazaki, M., Takaishi, M., Sakaguchi, Y., Makino, E., Kataoka, N., Yamada, H., Namba, M., and Huh, N. H.:** S100C/A11 is a key mediator of Ca(2+)-induced growth inhibition of human epidermal keratinocytes. J. Cell Biol., **163**, 825–835 (2003).
41. **Gahmberg, C. G. and Tolvanen, M.:** Why mammalian cell surface proteins are glycoproteins. Trends Biochem. Sci., **248**, 308–311 (1996).
42. **Varki, A.:** Metabolic radiolabeling of glycoconjugates. Methods Enzymol., **230**, 16–32 (1994).
43. **Reuter, G. and Schauer, R.:** Determination of sialic acids. Methods Enzymol., **230**, 168–199 (1994).
44. **Futami, J., Tsushima, Y., Tada, H., Seno, M., and Yamada, H.:** Convenient and efficient *in vitro* folding of disulfide-containing globular protein from crude bacterial inclusion bodies. J. Biochem. (Tokyo), **127**, 435–441 (2000).

Antiangiogenic agent SU6668 suppresses the tumor growth of xenografted A-431 cells

TAKESHI NAKAMURA, SOJI OZAWA, YUKO KITAGAWA, MASAKAZU UEDA, TETSURO KUBOTA and MASAKI KITAJIMA

Department of Surgery, School of Medicine, Keio University, Tokyo, Japan

Received June 30, 2005; Accepted August 17, 2005

Abstract. SU6668 is an antiangiogenic agent that acts as a tyrosine kinase inhibitor for the vascular endothelial growth factor (VEGF) receptor. We treated xenografted A-431, a human squamous cell carcinoma cell line, with SU6668 to investigate the efficacy of tumor dormant therapy using angiogenesis inhibitors for patients with squamous cell carcinoma. A-431 cells were transplanted into severe combined immunodeficient (SCID) mice. The treatment group was given SU6668 at a dose of 200 mg/kg orally twice a day for 3 weeks; the control group was given only the vehicle in the same manner and intervals. SU6668 suppressed tumor growth of A-431 cells in the xenograft model. Furthermore, tumor volume and the number of vessels were significantly reduced in the treatment group compared with those of the control. No significant differences in body weight were found between the treatment and control groups, and no toxic reactions occurred during the experiment. We concluded that this agent was safe, efficient and potentially useful for the treatment of patients with squamous cell carcinoma.

Introduction

The prognosis of patients with esophageal cancer is dismal (1). Although advances in esophageal cancer therapy, including surgical technique and chemoradiation therapy, have been remarkable, the 5-year survival rate for patients undergoing curative or palliative resection is 40.0-42.4% (2,3). The majority of patients with esophageal cancer in Japan have squamous cell carcinoma. New paradigms and therapeutic approaches, such as antiangiogenic therapy, need to be investigated to improve the treatment of this neoplasm.

Tumor angiogenesis is essential for the tumor growth and metastatic spread of several solid tumors (4), and is induced by several angiogenic growth factors. Among several dozen angiogenic growth factors identified thus far, vascular endothelial growth factor (VEGF), fibroblast growth factor (FGF), and platelet-derived growth factor (PDGF) have been widely studied and reported. These angiogenic growth factors are related to poor prognosis in some solid tumors (5-10), and we have also reported that VEGF expression is associated with a poor outcome and lymph node metastasis in squamous cell carcinoma of the esophagus (11). The inhibition of angiogenesis is expected to play a key role in the treatment of squamous cell carcinoma. Numerous small molecules and biological agents capable of inhibiting tumor-induced vascularization, like marimastat, BMS275291, BAY12-9566, neovastat, SU5416, SU6668, and ZD6474, have been identified (12-18). We hypothesized that angiogenesis inhibitors targeting VEGF, might also be applicable as a tumor dormant therapy for patients with squamous cell carcinoma. SU6668, (z)-3-[2,4-dimethyl-5-(2-dihydro-3-ylidenemethyl)-1H-pyrrol-3-yl]-propionic acid, a small molecule, is a relatively broad-spectrum receptor tyrosine kinase inhibitor that inhibits the function of the VEGF, FGF and PDGF receptors (19). This agent affects tumor vascularization and the growth of some types of xenografts (13,19,20). A-431 is a squamous cell carcinoma cell line that can be implanted into severe combined immunodeficient (SCID) mice. Here, we examined the antitumor effects of SU6668 on squamous cell carcinoma xenografts of A-431 in SCID mouse to test our hypothesis.

Materials and methods

Cell line. A-431 cells were obtained from Riken (Tsukuba, Japan). The A-431 tumor cell line was successfully transplanted into SCID mice in our laboratory. Cells from an early generation were stored in liquid nitrogen, and new cultures were established every 2-3 months.

Mice. Severe combined immunodeficient (SCID) mice with a genetic background of BALB/c were obtained from the Saitama Laboratory Animal Center (Saitama, Japan). All mice were maintained under specific pathogen-free conditions using an isorack in our experimental animal center and fed sterile food and water *ad libitum*. The 4-week-old male mice weighing 20-22 g each (n=10) were used in the study. The mice were randomly placed in a control (n=5) or SU6668 treatment (n=5) group. All animal studies were conducted according to institutional guidelines approved by the Animal Care and Use Committee of our university.

Correspondence to: Dr Soji Ozawa, Department of Surgery, School of Medicine, Keio University, Shinjuku-ku, Tokyo 160-8582, Japan
E-mail: ozawa@sc.itc.keio.ac.jp

Key words: squamous cell carcinoma, angiogenesis, A-431, SU6668, xenograft model

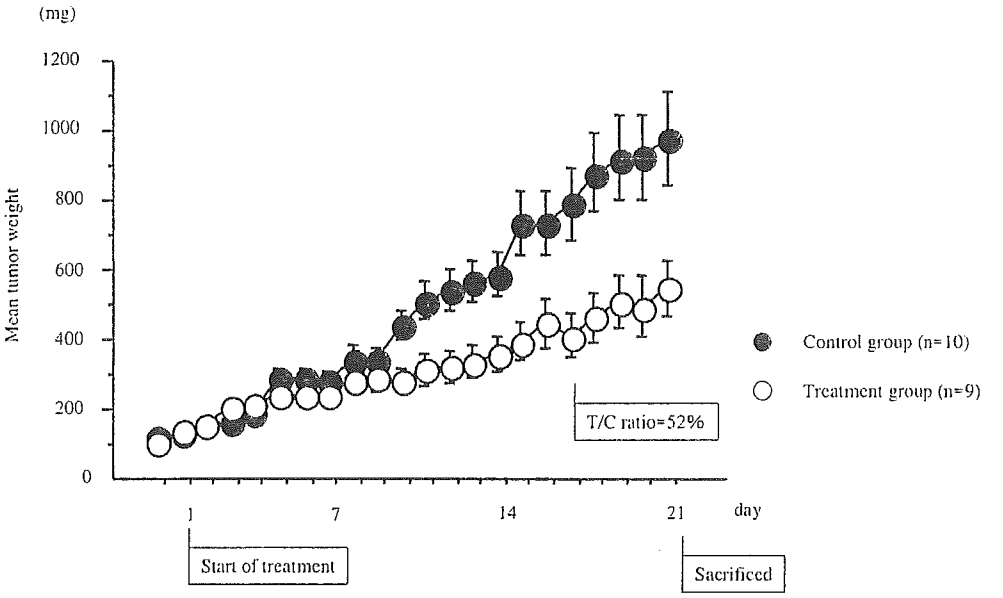

Figure 1. Antitumor activity of SU6668 against A-431 tumor cells transplanted into SCID mice. Tumor growth was suppressed in the treatment groups from 10 days after treatment until the end of the experiment. The T/C ratio was 52% at 17 and 18 days.

Reagents and antibodies. SU6668, (z)-3-[2,4-dimethyl-5-(2-dihydro-3-ylidenemethyl)-1H-pyrrol-3-yl]-propionic acid, was provided by Taiho Pharmaceutical Co., Ltd., Tokyo, Japan. SU6668 was formulated at a concentration of 50 mg/ml in an aqueous-base cremophor vehicle [16.92% 1 N sodium hydroxide solution, 24.6% cremophor EL (polyxyethylated caster oil), 1.56% benzyl alcohol, 35.14% PEG 400, and 16.79% deionized water]. To immunohistochemically quantify the tumor vessel counts, a monoclonal murine anti-human endothelial cell antibody, CD31 (clone JC/70A), was purchased from Dako (Denmark).

Tumor inoculation, measurement of tumor size and evaluation of agent activity. Initially, $1x10^7$ A-431 cells were implanted into SCID mice in our laboratory. After tumor formation, the tumor was resected and a single fragment of tumor tissue, measuring approximately 3 x 3 x 3 mm, was inoculated into the subcutaneous tissue of the bilateral dorsum of ether-anesthetized mice using a trocar needle. The resultant tumors were measured (length and width) daily using sliding calipers by the same observer. Tumor weight was calculated according to the method of Geran *et al* using linear measurements and the formula: tumor weight (mg) = length (mm) x [width (mm)]^2 x0.5 (21). On day 5 after tumor inoculation, when the tumors reached 100 to 300 mg, tumor-bearing mice were randomly allocated to test groups each consisting of 5 mice, and treatment was initiated.

The treatment group was given SU6668 at a dose of 200 mg/kg p.o. twice a day starting 5 days after transplantation for 21 days, while the control group was given only the vehicle. Animals were sacrificed 26 days after the initial treatment. The mice were sacrificed by cervical dislocation after adequate sedation with methoxyflurane had been confirmed using the toe pinch technique. The tumors were then excised and weighed. For CD31 staining, a section of the tumor tissue was fixed using the acetone-methylbenzoate-xylene (Amex) method and an immunohistochemical analysis was performed.

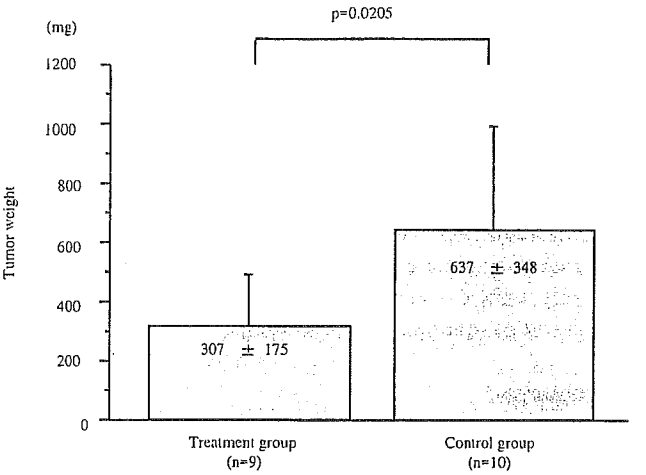

Figure 2. Actual tumor weight at the time of sacrifice. The mean tumor weight of the treatment groups (307±175 mg) was significantly lower (p=0.0205) than that of the control groups (637±348 mg).

The antitumor effects of treatments were assessed by evaluating the inhibition rate and calculated using the formula: 100 - lowest T/C value (%) during the experiment, where T is the relative mean tumor weight of the treated group and C is the relative mean tumor weight of the control group at any given time. The presence of antitumor activity was defined as an inhibition rate ≥58%; this cutoff value was determined using the value of $1-(0.75)^3$, which corresponds to a 25% reduction in tumor diameter (22).

Immunohistochemical analysis. To quantify the tumor vessel counts, immunohistochemical staining was performed using the AmeX method (23). Tissue specimens were fixed in acetone at -20°C overnight. The specimens were dehydrated in acetone at 4°C for 15 min, again at room temperature for 15 min, and rinsed twice in methyl benzoate and xylene at room temperature for 15 min. Tissues were permeated with paraffin at 60°C for 3 h, then embedded in paraffin and cut

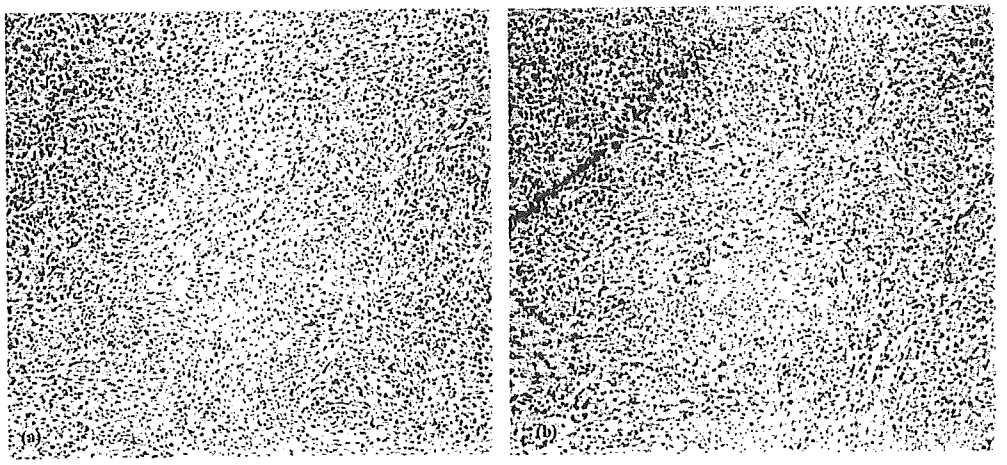

(a) Treatment group (b) Control group

Figure 3. Immunohistochemical staining for CD31. Endothelial cells were positively stained. (a) Treatment group and (b) control group.

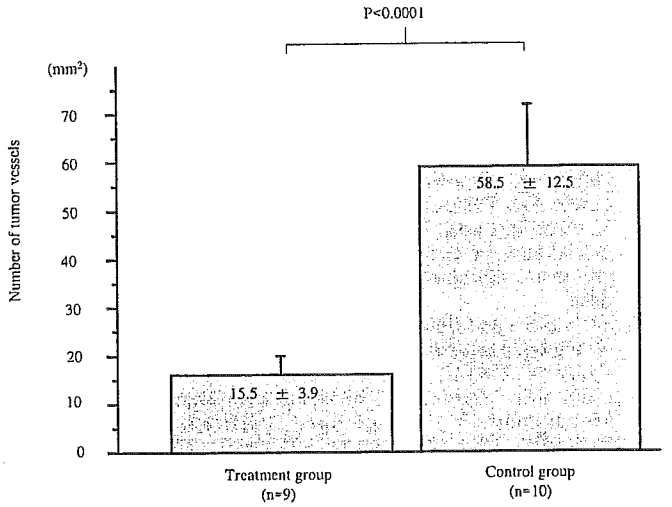

Figure 4. Number of tumor vessels. The mean density of tumor vessels in the treatment group (15.5±3.9/mm²) was significantly lower than that in the control group (58.5±12.5/mm²) ($p<0.0001$).

into 4-μm sections for immunohistochemistry with primary antibodies to CD31 (endothelial cells). Five random 0.159-mm² fields at a x100 magnification were captured for each tumor using light microscopy.

Statistical analysis. Tumor volume, body weight, tumor weight and tumor vessel density were compared between the two groups using an unpaired Student's t-test. Statistical significance was defined as $p<0.05$.

Results

Toxicity. Treatment toxicity was monitored by observing the loss of animal body weight. No significant differences in body weight were found between the treatment and control groups, and no toxic reactions occurred. No deaths or body weight loss >4.3% were seen in either the control or treated mice during the experiment.

Effect on tumor growth. Fig. 1 shows the suppression of A-431 tumor growth by SU6668 in SCID mice. Relative to the control mice, the mean tumor volumes were smaller in the treatment groups from 10 days after treatment until the end of the experiment, with a T/C ratio of 52% at 17 and 18 days after treatment. However, SU6668 significantly reduced the actual tumor weight (637 mg in the control group and 308 mg in the SU6668 group; $p=0.02$) (Fig. 2).

Effect on tumor angiogenesis. We assessed tumor angiogenesis using immunohistochemical staining for CD31 to detect vessels in the tumors (Fig. 3). The density of tumor vessels in the treatment group (15.5/mm²) was significantly lower ($p<0.0001$) than that in the control group (58.5/mm²) (Fig. 4).

Discussion

In this study, we found that the daily oral administration of SU6668 significantly suppressed the growth of A-431 tumors in SCID mouse. While the mean relative tumor ratio was >48%, the actual tumor weight of the treatment group was statistically lower than that of the control group.

The suppression of tumor growth caused by daily treatment with SU6668 was apparently related to a marked decline in blood perfusion in the tumor. In this study, the number of tumor vessels in the treatment group was significantly fewer than that in the control group. Previous studies have shown that SU6668 inhibits tumor growth in mice by inhibiting the proliferation of vascular endothelial cells and inducing apoptosis (19,20). The SU6668-induced inhibition of angiogenic receptor tyrosine kinase activity is associated with rapid vessel killing in tumors, leading to broad and potent antitumor effects (24). Our results confirmed those of previous reports, providing further evidence that the inhibition of angiogenesis-related receptor tyrosine kinase activity suppresses tumor growth, and SU6668 suppresses tumor growth through its inhibitory effects on tumor angiogenesis.

No significant differences in body weight were found between the treatment and control groups, and no toxic reactions occurred during the experiment. As none of the mice died during the experiment, the adverse effects of this

agent appear to be minimal. Angiogenesis inhibitors target angiogenic endothelial cells and are not likely to produce or exacerbate either local or systemic toxicity caused by radiotherapy and chemotherapy (25). The appearance of antiangiogenic drugs has caused a paradigm shift in approaches to cancer therapy, and cancer can now be considered a 'chronic disease' because antiangiogenic therapy may keep patients alive with a minimal tumor load (26). Antiangiogenic drugs are also expected to change current strategies for cancer therapy.

Another strategy to increase the efficacy of antiangiogenic therapy is to combine antiangiogenic agents with conventional cytotoxic therapies, such as radiation therapy and chemotherapy (27). SU6668, a potent therapeutic agent, is potentially useful for suppressing tumor growth and enhancing the response of tumors to radiotherapy (26,28). An increase in response by tumors to radiation after exposure to SU6668 may improve the efficacy of chemoradiation therapy in patients with squamous cell carcinoma. Furthermore, combined antiangiogenic and immune therapy may represent a new strategy for cancer treatment (29). Xiong *et al* reported that it was feasible to conduct a phase I trial of SU6668 using functional computed tomography scans and dynamic contrast enhanced magnetic resonance imaging (DCE-MRI) (30). DCE-MRI is a promising approach to non-invasively monitor the sequence of vascular events that occur during tumor growth, making it useful for characterizing the activity of antiangiogenic and vascular targeting agents (31). Some studies have also suggested that SU6668 inhibits peritoneal dissemination and prolongs survival in mouse models (32,33). We conclude that SU6668 is safe, efficient and potentially useful for the treatment of squamous cell carcinoma, and may in the near future change treatment strategies for patients with squamous cell carcinoma.

Acknowledgements

The authors wish to thank Dr Eiji Ikeda for his technical advice regarding the immunohistochemical staining and Ms. Yuki Inaba for her expert technical assistance.

References

1. Lerut T, Deleyn P, Coosemans W, *et al*: Surgical strategies in esophageal carcinoma with emphasis on radical lymphadenectomy. Ann Surg 216: 583-590, 1992.
2. Akiyama H, Tsurumaru M, Udagawa H and Kajiyama Y: Radical lymph node dissection for cancer of the thoracic esophagus. Ann Surg 220: 364-373, 1994.
3. Ando N, Ozawa S, Kitagawa Y, Shinozawa Y and Kitajima M: Improvement in the results of surgical treatment of advanced squamous esophageal carcinoma during 15 consecutive years. Ann Surg 232: 225-232, 2000.
4. Folkman J: What is the evidence that tumors are angiogenesis dependent? J Natl Cancer Inst 82: 4-6, 1990.
5. Takanami I, Imamura T, Hashizume T, Kikuchi K, Yamamoto Y, Yamamoto T and Kodaira S: Immunohistochemical detection of basic fibroblast growth factor as a prognostic indicator in pulmonary adenocarcinoma. Jpn J Clin Oncol 26: 293-297, 1996.
6. Takebayashi Y, Miyadera K, Akiyama S, Hokita S, Yamada K, Akiba S, Yamada Y, Sumizawa T and Aikou T: Expression of thymidine phosphorylase in human gastric carcinoma. Jpn J Cancer Res 87: 288-295, 1996.
7. Maeda K, Kang SM, Ogawa M, Onoda N, Sawada T, Nakata B, Kato Y, Chung YS and Sowa M: Combined analysis of vascular endothelial growth factor and platelet-derived endothelial cell growth factor expression in gastric carcinoma. Int J Cancer 74: 545-550, 1997.
8. Li Z, Shimada Y, Uchida S, Maeda M, Kawabe A, Mori A, Itami A, Kano M, Watanabe G and Imamura M: TGF-α as well as VEGF, PD-ECGF and bFGF contribute to angiogenesis of esophageal squamous cell carcinoma. Int J Oncol 17: 453-460, 2000.
9. Kuwahara K, Sasaki T, Kuwada Y, Murakami M, Yamasaki S and Chayama K: Expression of angiogenic factors in pancreatic ductal carcinoma. A correlative study with clinicopathologic parameters and patient survival. Pancreas 26: 344-349, 2003.
10. Kaio E, Tanaka S, Kitadai Y, Sumii M, Yoshihara M, Haruma K and Chayama K: Clinical significance of angiogenic factor expression at the deepest invasive site of advanced colorectal carcinoma. Oncology 64: 61-73, 2003.
11. Shih CH, Ozawa S, Ando N, Ueda M and Kitajima M: Vascular endothelial growth factor expression predicts outcome and lymph node metastasis in squamous cell carcinoma of the esophagus. Clin Cancer Res 6: 1161-1168, 2000.
12. Wojtowicz-Praga SM, Dickson RB and Hawkins MJ: Matrix metalloproteinase inhibitors. Invest New Drugs 15: 61-75, 1997.
13. Fong TA, Shawver LK, Sun L, Tang C, App H, Powell TJ, Kim YH, Schreck R, Wang X, Risau W, Ullrich A, Hirth KP and McMahon G: SU5416 is a potent and selective inhibitor of the vascular endothelial growth factor receptor (Flk-1/KDR) that inhibits tyrosine kinase catalysis, tumor vascularization, and growth of multiple tumor types. Cancer Res 59: 99-106, 1999.
14. Erlichman C, Adjei AA, Alberts SR, Sloan JA, Goldberg RM, Pitot HC, Rubin J, Atherton PJ, Klee GG and Humphrey R: Phase I study of the matrix metalloproteinase inhibitor, BAY 12-9566. Ann Oncol 12: 389-395, 2001.
15. Falardeau P, Champagne P, Poyet P, Hariton C and Dupont E: Neovastat, a naturally occurring multifunctional antiangiogenic drug, in phase III clinical trials. Semin Oncol 28: 620-625, 2001.
16. Hoekman K: SU6668, a multitargeted angiogenesis inhibitor. Cancer J 7: S134-138, 2001.
17. Naglich JG, Jure-Kunkel M, Gupta E, Fargnoli J, Henderson AJ, Lewin AC, Talbott R, Baxter A, Bird J, Savopoulos R, Wills R, Kramer RA and Trail PA: Inhibition of angiogenesis and metastasis in two murine models by the matrix metalloproteinase inhibitor, BMS-275291. Cancer Res 61: 8480-8485, 2001.
18. Sridhar SS and Shepherd FA: Targeting angiogenesis: a review of angiogenesis inhibitors in the treatment of lung cancer. Lung Cancer 42: S81-91, 2003.
19. Laird AD, Vajkoczy P, Shawver LK, Thurnher A, Liang C, Mohammadi M, Schlessinger J, Ullrich A, Hubbard SR, Blake RA, Fong TA, Strawn LM, Sun L, Tang C, Hawtin R, Tang F, Shenoy N, Hirth KP, McMahon G and Cherrington JM: SU6668 is a potent antiangiogenic and antitumor agent that induces regression of established tumors. Cancer Res 60: 4152-4160, 2000.
20. Shaheen RM, Davis DW, Liu W, Zebrowski BK, Wilson MR, Bucana CD, McConkey DJ, McMahon G and Ellis LM: Antiangiogenic therapy targeting the tyrosine kinase receptor for vascular endothelial growth factor receptor inhibits the growth of colon cancer liver metastasis and induces tumor and endothelial cell apoptosis. Cancer Res 59: 5412-5416, 1999.
21. Geran RI, Greenberg NH, Macdonald MM, Schumacher AM and Abott BJ: Protocols for screening chemical agents and natural products against animal tumors and other biological systems (3rd edition). Cancer Chemother Rep 3: 51-61, 1972.
22. Kubota T, Nakada M, Tsuyuki K, Ishibashi K and Abe O: Cell kinetics and chemosensitivity of human carcinoma serially transplanted into nude mice. Jpn J Cancer Res 77: 502-507, 1986.
23. Sato Y, Mukai K, Watanabe S, Goto M and Shimosato Y: The AmeX method; a simplified technique of tissue processing and paraffin embedding with improved preservation of antigens for immunostaining. Am J Pathol 125: 431-435, 1986.
24. Laird AD, Christensen JG, Li G, Carver J, Smith K, Xin X, Moss KG, Louie SG, Mendel DB and Cherrington JM: SU6668 inhibits Flk-1/KDR and PDGFRbeta *in vivo*, resulting in rapid apoptosis of tumor vasculature and tumor regression in mice. FASEB J 16: 681-690, 2002.
25. Ning S, Laird D, Cherrington JM and Knox SJ: The antiangiogenic agents SU5416 and SU6668 increase the antitumor effects of fractionated irradiation. Radiat Res 157: 45-51, 2002.
26. Lu B, Geng L, Musiek A, Tan J, Cao C, Donnelly E, McMahon G, Choy H and Hallahan DE: Broad spectrum receptor tyrosine kinase inhibitor, SU6668, sensitizes radiation via targeting survival pathway of vascular endothelium. Int J Radiat Oncol Biol Phys 58: 844-850, 2004.

27. Garofalo A, Naumova E, Manenti L, Ghilardi C, Ghisleni G, Caniatti M, Colombo T, Cherrington JM, Scanziani E, Nicoletti MI and Giavazzi R: The combination of the tyrosine kinase receptor inhibitor SU6668 with paclitaxel affects ascites formation and tumor spread in ovarian carcinoma xenografts growing orthotopically. Clin Cancer Res 9: 3476-3485, 2003.
28. Griffin RJ, Williams BW, Wild R, Cherrington JM, Park H and Song CW: Simultaneous inhibition of the receptor kinase activity of vascular endothelial, fibroblast, and platelet-derived growth factors suppresses tumor growth and enhances tumor radiation response. Cancer Res 62: 1702-1706, 2002.
29. Huang X, Wong MK, Yi H, Watkins S, Laird AD, Wolf SF and Gorelik E: Combined therapy of local and metastatic 4T1 breast tumor in mice using SU6668, an inhibitor of angiogenic receptor tyrosine kinases, and the immunostimulator B7.2-IgG fusion protein. Cancer Res 62: 5727-5735, 2002.
30. Xiong HQ, Herbst R, Faria SC, Scholz C, Davis D, Jackson EF, Madden T, McConkey D, Hicks M, Hess K, Charnsangavej CA and Abbruzzese JL: A phase I surrogate endpoint study of SU6668 in patients with solid tumors. Invest New Drugs 22: 459-466, 2004.
31. Marzola P, Degrassi A, Calderan L, Farace P, Crescimanno C, Nicolato E, Giusti A, Pesenti E, Terron A, Sbarbati A, Abrams T, Murray L and Osculati F: *In vivo* assessment of antiangiogenic activity of SU6668 in an experimental colon carcinoma model. Clin Cancer Res 10: 739-750, 2004.
32. Machida S, Saga Y, Takei Y, Mizuno I, Takayama T, Kohno T, Konno R, Ohwada M and Suzuki M: Inhibition of peritoneal dissemination of ovarian cancer by tyrosine kinase receptor inhibitor SU6668 (TSU-68). Int J Cancer 114: 224-229, 2005.
33. Tokuyama J, Kubota T, Saikawa Y, Yoshida M, Furukawa T, Otani Y, Kumai K and Kitajima M: Tyrosine kinase inhibitor SU6668 inhibits peritoneal dissemination of gastric cancer via suppression of tumor angiogenesis. Anticancer Res 25: 17-22, 2005.

Expression of basic fibroblast growth factor is associated with a good outcome in patients with squamous cell carcinoma of the esophagus

TAKESHI NAKAMURA, SOJI OZAWA, YUKO KITAGAWA, CHIH-HORNG SHIH, MASAKAZU UEDA and MASAKI KITAJIMA

Department of Surgery, School of Medicine, Keio University, Tokyo, Japan

Received February 7, 2005; Accepted March 29, 2005

Abstract. Angiogenesis is an essential step in tumor growth and metastasis, but rather than being controlled by means of a simple mechanism, the control of tumor angiogenesis may be mediated by several angiogenic factors. We investigated the expression of basic fibroblast growth factor (b-FGF) and platelet-derived endothelial cell growth factor (PD-ECGF) in squamous cell carcinoma of the esophagus in order to clarify the mechanism of angiogenesis. Expression of b-FGF and PD-ECGF was immunohistochemically investigated in tissue specimens from the tumors of 79 patients with squamous cell carcinoma of the esophagus who underwent curative esophagectomy without preoperative chemotherapy or radiation therapy, and the relationship between expression of b-FGF/PD-ECGF, microvessel density (MVD), and clinicopathological background factors was assessed. Tumor cells that expressed b-FGF were found in 41 patients (51.9%), and tumor cells that expressed PD-ECGF were found in 57 patients (72.2%). Although the mean vascular density (47.9/mm^2) of b-FGF-positive tumors was significantly lower than that (67.2/mm^2) of b-FGF-negative tumors (p=0.014), the difference between the 56.0/mm^2 in PD-ECGF-positive tumors and 60.3/mm^2 in PD-ECGF-negative tumors was not significant. Although the survival rate of patients with b-FGF-positive tumors was significantly higher than those with b-FGF-negative tumors (p=0.033), there was no significant difference between the survival rates of patients with PD-ECGF-positive and -negative tumors (p=0.580). Expression of b-FGF may be associated with promotion of angiogenesis and a good prognostic factor in squamous cell carcinoma of the esophagus.

Introduction

Previous studies have demonstrated that the development of microvessels in solid tumors plays a key role in tumor growth and angiogenesis contributes to tumor invasion and metastasis (1). We have reported a significantly higher survival rate in patients with squamous cell carcinoma of the esophagus who have low-MVD (microvessel density) tumors than in patients with high-MVD tumors (2). The higher the vascular density of the tumor, the worse the outcome. We have also reported that vascular endothelial growth factor (VEGF) is associated with the promotion of angiogenesis in squamous cell carcinoma of the esophagus, and angiogenesis seemed to be a significant prognostic factor (2). VEGF is likely to be a major regulator of angiogenesis, but rather than being controlled by VEGF alone, the control of tumor angiogenesis may be mediated by several angiogenic factors.

Basic-fibroblast growth factor (b-FGF) has been well characterized as an angiogenic factor (3,4) and is recognized as one of the most common angiogenic growth factors. Some studies have reported that b-FGF expression is associated with the promotion of angiogenesis and may be a prognostic factor for other solid tumors (5-7). Platelet-derived endothelial cell growth factor (PD-ECGF) is a thymidine phosphorylase and was initially purified as the major promotor of angiogenic activity in platelets (8-10). Previous studies have suggested that the expression of PD-ECGF is associated with increased angiogenesis, tumor vascularity, MVD, and lymph node metastasis in human gastric carcinoma, pancreatic ductal carcinoma, and colorectal carcinoma (11-14).

Turning on the angiogenic switch is a very early event in the development of invasive esophageal carcinoma, and advanced stage tumors show activation of various angiogenic pathways (15). It has been reported that cancer cell positivity for PD-ECGF is a predictor of good outcome in cervical squamous cell carcinoma treated with radiotherapy alone (16). Since tumor angiogenesis is a complicated process whose mechanisms remain unclear, we examined the relationship between expression of b-FGF/PD-ECGF and MVD, and clinicopathological background factors in squamous cell carcinoma of the esophagus.

Materials and methods

Clinical material. Tissue samples were obtained from the tumors of 79 patients with squamous cell carcinoma of the esophagus who underwent curative esophagectomy without preoperative chemotherapy or radiation therapy between

Correspondence to: Dr Soji Ozawa, Department of Surgery, School of Medicine, Keio University, Shinjuku-ku, 160-8582, Tokyo, Japan
E-mail: ozawa@sc.itc.keio.ac.jp

Key words: squamous cell carcinoma, basic-fibroblast growth factor, platelet-derived endothelial cell growth factor, prognosis

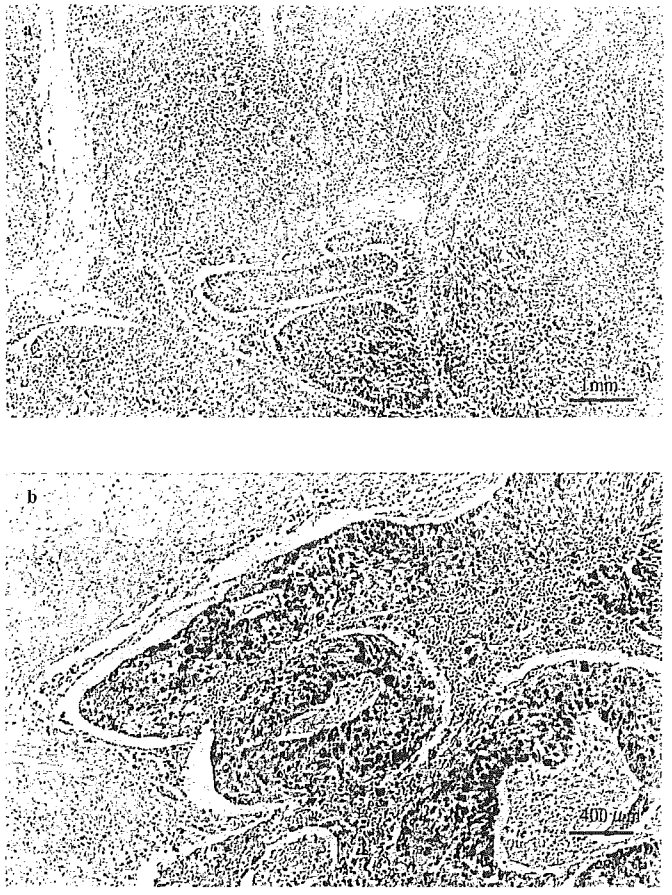

Figure 1. Immunohistochemical staining. (a) Immunohistochemical staining of a squamous cell carcinoma of the esophagus for b-FGF. Scale bar, 1 mm. (b) Immunohistochemical staining of a squamous cell carcinoma of the esophagus for PD-ECGF. Scale bar, 400 μm.

1990 and 1994 at Keio University Hospital (Tokyo, Japan). There were 73 male and 6 female patients, ranging in age from 40 to 83 years with an average age of 61.5 years. The maximum patient follow-up period was 149 months, and the median observation period was 80 months. Of the 79 patients, 52 who underwent esophagectomy and did not receive postoperative adjuvant therapy were selected for a life-table analysis. For convenience, we chose 60 months as the maximum period after surgery in the life-table analysis.

The microvessel density of these tissue samples had been calculated as described in our previous report (2). The tissues were fixed in phosphate-buffered 10% formalin at pH 7.4 and embedded in paraffin. Histopathologic examination was performed to determine the histological differentiation, depth of invasion, presence of lymph node metastasis, and lymphatic and venous invasion, according to the Guidelines for Clinical and Pathological Studies on Carcinoma of the Esophagus (17).

Immunohistochemical staining. After cutting 10-μm sections from 10% formalin-fixed, paraffin-embedded blocks from the most invasive area of carcinoma according to the pathology report and mounting them on slides, a labeled streptavidin biotin (LSAB) kit (Dako, Glostrup, Denmark) was used for immunohistochemical staining. DAB was used as the chromogen, and Mayer's hematoxylin as the counterstain.

Antibodies. The primary antibodies were an anti-b-FGF mouse monoclonal antibody (Wako) and 1C6-203, a mouse monoclonal antibody that recognizes PD-ECGF (Nippon Roche Research Center, Kanagawa, Japan). Normal mouse IgG was used as the primary antibody to provide a negative control. Vessel counts and VEGF expression were determined as described previously (2).

Staining analysis. The cytoplasm of cancer cells was examined for expression of b-FGF and PD-ECGF. Tumors were evaluated as positive if the cytoplasm of some cancer cells reacted positively.

Statistical analysis. The clinicopathological features and histochemical findings were analyzed with the Chi-square or Mann-Whitney test. Survival rates were retrospectively calculated using the Kaplan-Meier method and analyzed with the log-rank test based on the number of patients who died of the carcinoma. The influence of each variable on survival was assessed by Cox's proportional hazards regression model. Statistical significance was defined as $p<0.05$. All analyses were performed with a Macintosh computer (Apple Computer Inc., Cupertino, CA) and Statview statistic package (Abacus Concepts, Inc., Berkeley, CA).

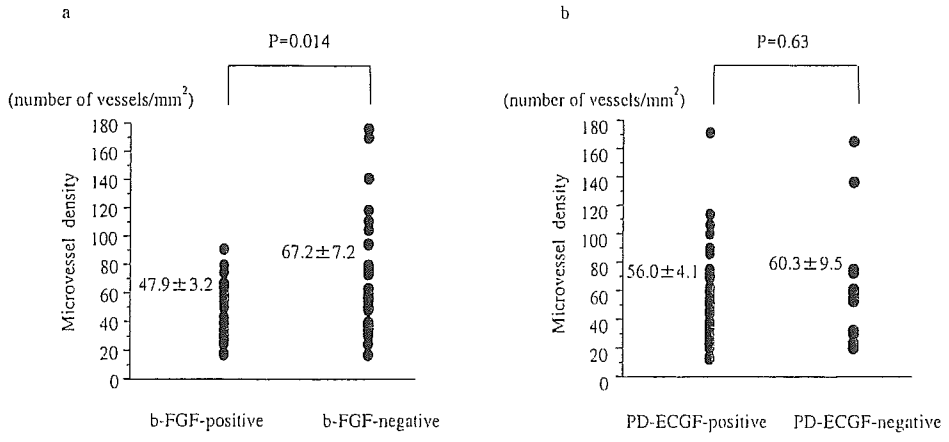

Figure 2. Microvessel density. (a) MVD of b-FGF-positive and -negative tumors. MVD was 47.9±3.2 (mean ± SE)/mm² in b-FGF-positive cases, and 67.2±7.2 /mm² in the b-FGF-negative cases (p=0.014). (b) MVD of PD-ECGF-positive and VEGF-negative tumors. There was no significant difference.

Table I. Relationship between b-FGF expression and clinicopathological factors.

	Positive (n=41)	Negative (n=38)	p-value
Age (years)			
≤49	3 (7.3%)	5 (13.3%)	NS
50-59	17 (41.5%)	9 (23.6%)	
60-69	17 (41.5%)	15 (39.5%)	
≥70	4 (19.8%)	9 (23.6%)	
Sex			
Male	37 (90.2%)	36 (94.7%)	NS
Female	4 (9.8%)	2 (5.3%)	
Location			
Upper	6 (14.6%)	5 (13.2%)	NS
Middle	20 (45.5%)	21 (55.3%)	
Lower	15 (36.6%)	12 (31.6%)	
Adjuvant therapy			
None	26 (63.4%)	26 (68.4%)	NS
Radiation therapy	1 (2.4%)	3 (7.9%)	
Chemotherapy	12 (29.3%)	8 (21.1%)	
pT-Factor			
1	11 (26.8%)	8 (21.1%)	NS
2	4 (9.8%)	7 (18.4%)	
3	26 (63.4%)	23 (60.5%)	
pN-Factor			
0	8 (19.5%)	14 (36.8%)	NS
1	33 (80.5%)	24 (63.2%)	
Histological type			
Well-differentiated	9 (22.0%)	5 (13.2%)	NS
Moderately differentiated	31 (75.6%)	32 (84.2%)	
Poorly differentiated	1 (2.4%)	1 (2.6%)	
Infiltrative growth pattern			
Inf-α	3 (7.3%)	2 (5.3%)	NS
Inf-ß	36 (87.8%)	33 (86.8%)	
Inf-γ	1 (2.4%)	3 (7.9%)	
Lymphatic invasion			
(-)	5 (12.2%)	6 (15.8%)	NS
(+)	36 (87.8%)	32 (84.2%)	
Vessel invasion			
(-)	10 (24.4%)	11 (28.9%)	NS
(+)	31 (75.6%)	27 (71.1%)	

NS, not significant.

Results

b-FGF and PD-ECGF were not immunohistochemically detected in normal esophageal epithelium. Expression of b-FGF and PD-ECGF was identified mainly in the cytoplasm of tumor cells (Fig. 1). Of 79 cases 41 (51.9%) were evaluated as b-FGF-positive, and 57 (72.2%) as PD-ECGF-positive. There were no significant differences in any of the clinicopathological variables between the positive and negative groups (Tables I and II).

MVD was significantly lower in b-FGF-positive tumors (47.9±3.2/mm^2) than b-FGF-negative tumors (67.2±7.2/mm^2) (p=0.014). MVD was 56.0±4.1/mm^2 in PD-ECGF-positive tumors and 60.3±9.5/mm^2 in PD-ECGF-negative tumors; the difference was not statistically significant (Fig. 2).

Table II. Relationship between PD-ECGF expression and clinicopathological factors.

	Positive (n=57)	Negative (n=22)	p-value
Age (years)			
≤49	4 (7%)	4 (18.2%)	NS
50-59	19 (33.3%)	7 (31.8%)	
60-69	25 (43.9%)	7 (31.8%)	
≥70	9 (15.8%)	4 (18.2%)	
Sex			
Male	54 (94.7%)	19 (86.4%)	NS
Female	3 (5.3%)	3 (13.6%)	
Location			
Upper	8 (14%)	3 (13.6%)	NS
Middle	26 (45.6%)	15 (68.2%)	
Lower	23 (40.4%)	4 (18.2%)	
Adjuvant therapy			
None	36 (66.7%)	16 (77.2%)	NS
Radiation therapy	2 (3.7%)	1 (4.5%)	
Chemotherapy	16 (28.1%)	4 (18.2%)	
pT-Factor			
1	15 (26.3%)	4 (18.2%)	NS
2	7 (12.3%)	4 (18.2%)	
3	35 (61.4%)	14 (63.6%)	
pN-Factor			
0	13 (22.8%)	9 (40.9%)	NS
1	44 (77.2%)	13 (59.1%)	
Histological type			
Well-differentiated	10 (17.5%)	4 (18.2%)	NS
Moderately differentiated	45 (78.9%)	18 (81.8%)	
Poorly differentiated	2 (3.5%)	0 (0%)	
Infiltrative growth pattern			
Inf-α	3 (5.3%)	2 (9.1%)	NS
Inf-ß	51 (89.5%)	19 (86.4%)	
Inf-γ	3 (5.3%)	1 (4.5%)	
Lymphatic invasion			
(-)	6 (10.5%)	4 (18.2%)	NS
(+)	51 (89.5%)	18 (81.8%)	
Vessel invasion			
(-)	16 (28.1%)	5 (22.7%)	NS
(+)	41 (71.9%)	17 (77.3%)	

NS, not significant.

The average number of metastatic lymph nodes at surgery was 3.3 in b-FGF-positive cases and 4.6 in b-FGF-negative cases (p=0.275), and 4.7 in PD-ECGF-positive cases and 2.0 in PD-ECGF-negative cases (p=0.055) (Fig. 3).

The cumulative survival rate of patients who underwent esophagectomy and did not receive postoperative chemotherapy was analyzed (n=52). The survival rate in b-FGF-positive cases was significantly higher than b-FGF-negative cases (p=0.033), but the survival rate in PD-ECGF-positive cases was not significantly different from that of PD-ECGF--negative cases (Fig. 4).

The prognostic value of b-FGF and PD-ECGF expression was compared with that of clinicopathological predictive factors, such as pT factor, pN factor, histological type, infiltrative growth pattern, and vessel invasion. The effects of variables presumed to be associated with outcome were

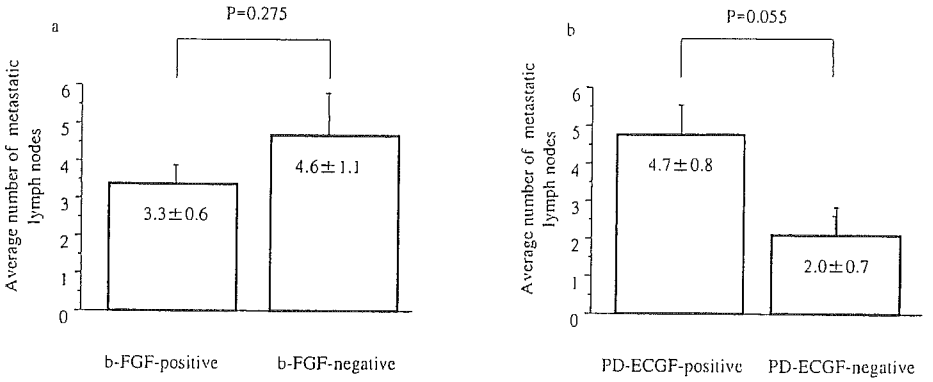

Figure 3. Average number of metastatic lymph nodes. (a) Number of metastatic lymph nodes in patients with b-FGF-positive and -negative tumors. (b) Number of metastatic lymph nodes in patients with PD-ECGF-positive and -negative squamous cell carcinoma of the esophagus. The number tended to be higher in PD-ECGF-positive cases than PD-ECGF-negative cases.

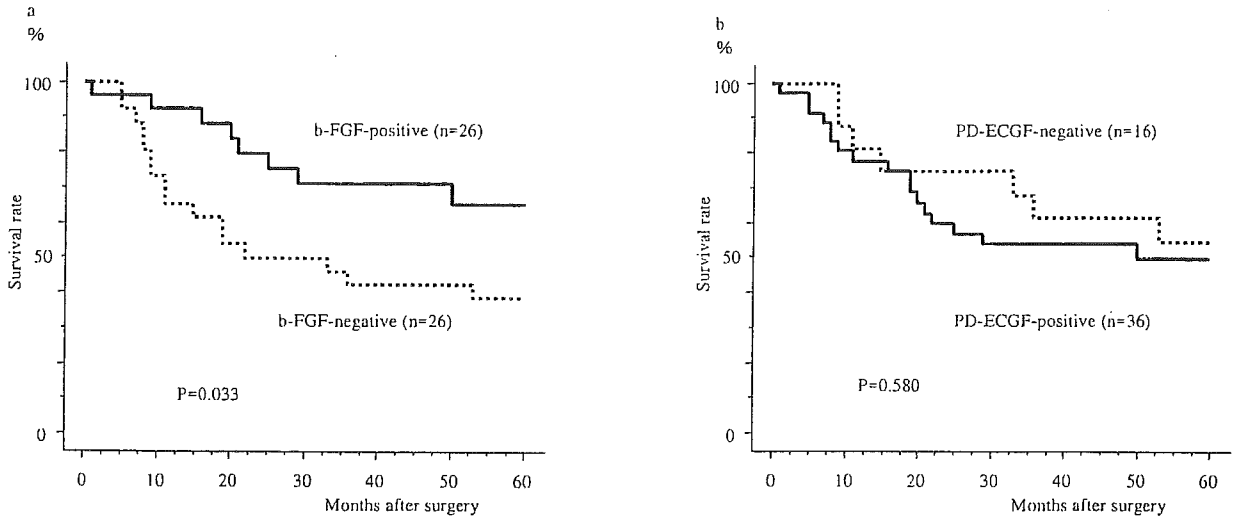

Figure 4. Survival curves after surgery without additional therapy. (a) Survival curves of b-FGF-positive and -negative cases after surgery without additional therapy. The survival rate of patients with b-FGF-positive tumors was significantly higher than that of patients with b-FGF-negative tumors (p=0.033). (b) The difference in survival rates between patients with PD-ECGF-positive tumors and -negative tumors was not significant (p=0.580).

Table III. Multivariate analysis with Cox's proportional hazards model.

Factors	Hazards ratio	p-value
b-FGF	7.183	0.0006
pN (0 or 1)	0.088	0.0014
PD-ECGF	0.301	0.0270
pT (1, 2 or 3)	2.120	0.1779
Vessel invasion	4.416	0.5500
Infiltrative growth pattern (α, ß or γ)	1.632	0.5529
Histological type (Well-, moderately or poorly differentiated)	1.771	0.6621

assessed by multivariate analysis using Cox's proportional hazards model, and the results showed the highest hazard ratio for b-FGF expression, and third highest hazard ratio for PD-ECGF expression (Table III).

Discussion

This retrospective study examined the relationship between expression of b-FGF/PD-ECGF, MVD, and clinicopathological background factors in squamous cell carcinoma of the esophagus. The results showed that b-FGF expression was associated with low MVD and a good outcome in patients with squamous cell carcinoma of the esophagus. Life-table analysis with Cox's proportional hazards model showed the highest hazard ratio for b-FGF expression, and the third highest hazard ratio for PD-ECGF expression. Both factors seemed to be associated with angiogenesis in squamous cell carcinoma of the esophagus.